10-047-009 (REV. 6/63)

DIVISION SNAP-8
TM 390:63-4-172
DATE 27 February 1964
W.O. 0740-33-2130
CR-72205

TECHNICAL MEMORANDUM

AUTHOR(S): R. A. Mendelson

TITLE: WELDED TRANSITION JOINTS OF 9Cr-1Mo ALLOY STEEL/316SS FOR SHORT LIFE (100 HOURS MAXIMUM) APPLICATION

ABSTRACT

Welding parameters and elevated temperature aging and strength characteristics of transition joints between 9Cr-1Mo alloy steel and 316 stainless steel were investigated. Three weld filler alloys were evaluated: 316L, 505, and Inco A.

Test capsules, each containing a transition joint, were fabricated from 1 in. OD x .109 in. wall tubing. They were subjected to 43 temperature/pressure cycles, and 1894 cumulative hours of exposure to pressure and/or temperature. All specimens completed the temperature/pressure test sequence without failure; however, one specimen failed in bend tests after exposure. Elevated temperature exposure produced carbon migration on joints fabricated using AISI 505 or 316L weld rod.

APPROVED:
DEPARTMENT HEAD R. S. Carey

NOTE: This document is considered preliminary and is subject to revision as analysis progresses and additional data are acquired. The general reader may encounter internal reference not available to him.

AEROJET-GENERAL CORPORATION

COPY NO.

I. INTRODUCTION

The SNAP-8 system contains interface joints between the mercury loop (9Cr-1Mo alloy steel) and the NaK loop (316 stainless steel). Data were available in the literature on methods of joining these materials; however, these joints have not been used at temperatures approaching the maximum of the SNAP-8 system, i.e.: 1325°F. To insure the reliability of a joint for a mercury boiler heat transfer test program requiring a minimum life of 100 hours, prototype joints were fabricated and evaluated under simulated boiler conditions.

II. PROCEDURE

Capsule test specimens were fabricated using 1 in. O.D. X .109 in. wall 9Cr-1Mo alloy steel and 316 stainless steel tubing. Tube sections were butt-welded using the TIG process. A "V" bevel groove joint (90° included angle) with a .032 in. land was employed. The fabrication procedure was as follows:

1. Preheat component parts to desired temperature. Preheat temperatures used were: 75°F, 400°F, or 600°F.
2. Complete root pass using no filler metal. Full penetration was required.
3. Complete welded joint using Inco A, AISI 505 (9Cr-1Mo steel), or 316L weld filler metal. Table I contains the nominal composition of these materials.
4. Weld an end plug of 9Cr-1Mo steel on the 9Cr-1Mo tube end and a standard 316 stainless steel 1/4 in. X 24 fitting on the 316 tube end.
5. Stress relieve capsule at 1350°F in air for 1/2 hour and air cool.
6. Dye penetrant and x-ray inspect all welds.

A complete test capsule is shown in Figure 1.

Twelve capsule specimens were made. They were identified by a two-digit number indicating welding parameters used. The designations are listed in Table 2. Three of these were duplicate capsules prepared using the three filler materials and 400°F preheat. These are identified by the prefix "R". One of these capsules, fabricated using AISI 505 filler, was rejected by x-ray inspection because of excessive porosity. It was discarded and was not replaced.

Bend and microhardness tests were conducted on longitudinal strips machined from capsules 60, 90, and A0, which were not exposed to the test environment. Metallographic samples were also taken from these as-fabricated capsules.

The bend tests are described as Test I in Table 3. The microhardness readings are recorded in Table 4. Photomicrographs are shown in Figures 2 through 5.

The remaining capsules completed a test program of temperature and temperature/pressure cycling. The capsules were placed in a radiant-heating furnace controlled to $\pm$ 10°F. Internal pressurization was achieved using argon gas fed through the AN fitting while the capsule was at temperature. The test sequence is summarized in Table 3.

After completion of Test 3, bend tests were run on longitudinal specimens machined from capsules R-64 and R-A4. The balance of the capsules concluded the test sequence. After completion of the final temperature/pressure cycling test, Test 7 (See Table 3), bend tests and metallographic and microhardness evaluation was performed.

The bend test is described as Test 8 in Table 3. A comparison of microhardness measurements on specimens before and after exposure is recorded in Table 4. Post-test photomicrographs are shown in Figures 6 through 12 with details in Figures 13 through 16.

III. TECHNICAL DISCUSSION

The test specimens containing 9Cr-1Mo/316 transition joints completed 43 temperature or temperature/pressure cycles and accumulated 1871 hours under a steady-state condition of combined temperature/pressure without failure. This would indicate that any of the filler alloys (316L, 505, or Inco A) would be suitable for welding 9Cr-1Mo/316 transition joints on components required to withstand 100 hours of testing.

The following five conditions developed at the transition joint during this evaluation program is as follows:

1. Weld Fusion Line Segregation
2. Decarburization
3. Hardness Increase
4. Grain Growth
5. Sensitization

These conditions may well impose a probable limit on anticipated life of these joints of less than 10,000 hours. A description and discussion of the import of each follows:

1. Weld Fusion Line Segregation:

Elevated temperature exposure of joints containing 316L or AISI 505 weld filler metal produced fusion line segregation at the interfaces of AISI 505/316 parent metal, AISI 505 filler/9Cr-1Mo parent metal, and 316L filler/9Cr-1Mo parent metal. This condition is shown in Figures 6, 7, and 8. The micro-constituents were identified by metallographic examination as a network of tempered martensite and excessive carbides. A comparison with specimen joints made using Inco A filler metal, see Figure 9, shows no such segregation.

The fusion line segregation is a plane of discontinuities which, in theory, is a potential plane of weakness at which localized or premature, yielding and subsequent failure may occur.

2. Decarubrization:

Elevated temperature exposure of joints containing 316L or AISI 505 weld filler metal produced decarburization of 9Cr-1Mo parent metal in the heat affected zones adjacent to the fusion line. This condition is apparent in Figures 8 and 11. The use of Inco A weld filler metal did not produce this effect, see Figure 9 and 10. Decarburization is caused by the migration of the carbon to carbide forming element, the 316L weld, an alloy which contains a larger percent of the chromium (18% Cr in 316L as opposed to 9% Cr in 9Cr-1Mo steel). Decarburization in the latter case (AISI 505 filler rod), occurred because of two reasons.

First, and of minor importance, the welding process created a condition favorable to carbon migration. A steep thermal gradient existed between the liquid weld filler metal and the unaffected preheated base metal. At some point immediately adjacent to the weld zone, a metal temperature was generated which produced a microstructural phase change in the 9Cr-1Mo steel from body centered cubic to face centered cubic. This temperature, known as Ac_1, is approximately $1500^{o}F$. The binary constitution diagram, Fe-C, shows the marked increase of solubility of carbon in the Fe face-centered cubic lattice structure over that of carbon in the Fe body-centered cubic lattice structure. Therefore, for the brief time during which the metal is in the former microstructural state (until it cools below the temperature at which retransformation occurs) an imbalance in the carbon equilibrium gradient at various points in the weld area is created. The AISI 505 filler material has a lower carbon content than the 9Cr-1Mo base material which would increase the carbon potential and allow carbon diffusion into the weld zone from the 9Cr-1Mo base material. Nickel is recognized as an effective barrier to carbon diffusion.[1] This explains the lack of decarburization in the 9Cr-1Mo steel heat affected zone in the specimens containing transition joints fabricated with the Inco A filler metal.

Second, and most important factor in the decarubrization of the 9Cr-1Mo steel, is the time at temperature.

A theoretical treatment carbon migration is included as Appendix A. It includes an explanation of the migration of carbon due to time at temperature.

The decarburized region would be much weaker than the adjacent area. A fatigue failure is possible when such a combination of structure is subjected to cyclic stress. When the decarburized region is adjacent to an area of higher hardness, the possibility of a shear failure is greatly increased.

3. Hardness Increase:

Elevated temperature exposure of the joints containing Inco A and AISI 505 weld filler metal resulted in a marked increase in the hardness of the weld metal. Table 4 compares the hardness of specimens before and after the exposure sequence described in Table 3. The hardness increase of the Inco A is attributed to age-hardening which is consistent with the titanium content of the alloy. No observed structural change can account for the hardness increase of the specimen containing AISI 505 weld filler metal.

The hardness increase is an indication of the brittleness of the joint and, similar to the consideration given to adjacent hard-soft areas produced by decarburization, it increases the possibility of a shear failure.

4. Grain Growth:

Elevated temperature exposure produced grain growth in the heat affected zone of the 316 stainless steel parent metal. Comparison of Figures 7 and 12, post-exposure photomicrographs, with Figure 3, pre-exposure photomicrograph, indicates the grain growth encountered.

There is some grain growth due to the heat input during welding. However, there is also growth due to extended exposure to high temperature during the test sequence described in Table 3. In comparing these pre- and post-test samples, some recrystallized 316 stainless steel grains are found to have formed at the fusion line as a result of test exposure. The driving force for the recrystallization appears to be the strain due to thermal stress imposed by cyclic heating and the strain due to the differences in thermal expansion between the 316 stainless steel and the 9Cr-1Mo alloy steel. The recrystallized grain grows to a larger size with time at elevated temperature during test exposure. In general, the large grain size will increase the resistance to creep, but will reduce the ability to elongate under stress.

5. Sensitization (Carbide Precipitation):

Exposure at 1325-1350°F produced sensitization of the 316L, 316SS, parent metal and heat affected zone. Figures 6 and 12 illustrate the sensitization (carbide precipitation) at grain boundaries in the 316SS parent metal and heat affected zones brought about by this exposure during the test sequence. The as-welded specimen, Figure 3, shows no sensitization. Sigma phase is also suspected as a microconstituent in the grain boundary in Figure 13. Comparison of specimens shows more carbide precipitation when the 9Cr-1Mo heat affected zone was decarburized. This effect is assumed to result from the additional free carbon made available by the migration.

The bend specimen which showed cracks in Test 8 (see Table 3), is shown macrographically in Figure 14. The crack occurred in the decarburized heat affected zone of the 9Cr-1Mo steel adjacent to a segregated fusion line, see Figure 15. Also, see details in Figure 16.

IV. CONCLUSIONS

1. The three weld filler materials tested are suitable for use in

making transition joints requiring moderate service life.

Five metallurgical unstable conditions were found in some of the samples after exposure. These conditions could limit useful lifetime to less than 10,000 hours.

IV. RECOMMENDATIONS

A program using 310 stainless steel weld filler should be initiated for transition joints between 9Cr-1Mo and 316 stainless steel. It is thought that the use of the 310 stainless steel will reduce or eliminate the problems encountered during exposure.

TABLE I

NOMINAL COMPOSITION OF MATERIALS

MATERIAL	WEIGHT - %										
	C	Mn	P	S	Si	Cr	Ni	Mo	Ti	Fe	Cu
9Cr-1Mo Steel	.15 max.	.30/ .60	.03 max.	.03 max.	.25/ 1.0	8.0/ 10.0	--	.90/ 1.10	--	Bal.	--
AISI 505 Weld Rod	.15 max.	.30/ .60	.03 max.	.03 max.	.25/ 1.0	8.0/ 10.0	--	.90/ 1.10	--	Bal.	--
316SS	.08 max.	2.0 max.	.045 max.	.03 max.	1.0 max.	16.00/18.00	10.00/14.00	2.0/3.0	--	Bal.	--
Filler 316L	.03 max.	2.0 max.	.045 max.	.03 max.	1.0 max.	16.00/18.00	10.00/14.00	2.0/3.0	--	Bal.	--
Inco Weld "A" (Now Inconel Filler Metal 92)	.03	2.20	--	.007	.10	16.4	71.5	---	3.1	6.70	.04

TABLE 2

IDENTIFICATION LEGEND FOR TEST CAPSULES

A.

CAPSULE IDENTIFICATION NUMBERS*

60	94
90	A4
A0	R-A4
64	66
R-64	96
	A6

B. LEGEND OF WELD PARAMETERS

DIGIT			
FIRST	SECOND	WELD FILLER MATERIAL	PREHEAT TEMP. °F
6		316L	
9		505	
A		Inco A	
	0		None
	4		400
	6		600

*Prefix (R) denotes duplicate specimen.

TABLE 3

TEST PROGRAM SEQUENCE

CAPSULE CONDITION, TEST VARIABLES AND RESULTS

TEST NO.	SPECIMEN NO.	FILLER MATERIAL	PREHEAT TEMP. °F	TEST CONDITIONS	CUMULATIVE EXPOSURE TIME	RESULTS - REMARKS
1	60 90 A0	316L 505 (9M) Inco A	75 (room) 75 (room) 75 (room)	Bend test around .250" radius through 180°		No failures
2	64 94 A4 66 96 A6	316L 505 (9M) Inco A 316L 505 (9M) Inco A	400 400 400 600 600 600	15 thermal cycles between 1325°F and room temperature	23 - temperature	No visible or measureable change.
3	Specimens from test #2 plus R-64 R-A4	See Test #2 316L Inco A	 400 400	14 thermal/pressure cycles between 1325°F/325 psig and room temp./0 psig	21 - temperature/pressure	No visual change
4	Specimens R-64 and R-A4 from test #3	See Test #3		Bend test around .250" radius through 180°		No failures or visual change
5	Specimens from test #2 used after completion of test #3	See Test #2		5 thermal/pressure cycles between 1325°F/325 psig and room temp./0 psig	171 - temperature/pressure	No failure or visual change
6	Specimens from test #2 used after completion of test #5	See Test #2		Continuous exposure at 1325°F and 325 psig	671 - temperature/pressure	No failures. No dimensional change noted.

(Continued - Page 2)

(TABLE 3 - Continued)

TEST NO.	SPECIMEN NO.	FILLER MATERIAL	PREHEAT TEMP. °F	TEST CONDITIONS	CUMULATIVE EXPOSURE TIME	RESULTS - REMARKS
7	Specimens from test #2 used after completion of test #6	See Test #2		8 thermal/pressure cycles between 1350°F/400 psig and room temp./0 psig	1871 - temperature/pressure	No visible change. No failures. .015" diameter growth (av.) of 9Cr-1Mo tube adjacent to weld.
8	Specimens from test #6 after completion of test #7	See Test #2		Bend test around .250" radius through 180°		Crack in specimen 66 at 150° bend. No other failures.

TABLE 4

MICROHARDNESS TRANSITION JOINTS - TEST RESULTS

AREA OF TEST	WELD FILLER MATERIAL INCO A	316L	AISI 505
Before Exposure:			
9Cr-1Mo Parent Metal	900-100 R_B	83-88 R_B	80-85 R_B
Weld Zone	81-88 R_B	36-37 R_C	84-88 R_B
316SS Parent Metal	83-91 R_B	83-94 R_B	73-80 R_B
After Exposure:			
9Cr-1Mo Parent Metal	72-74 R_B	74-75 R_B	72-77 R_B
Weld Zone	95-96 R_B	75-77 R_B	97-100 R_B
316SS Parent Metal	80-81 R_B	80 R_B	78 R_B

TRANSITION JOINT

9Cr-1Mo Alloy Steel

316 Stainless Steel

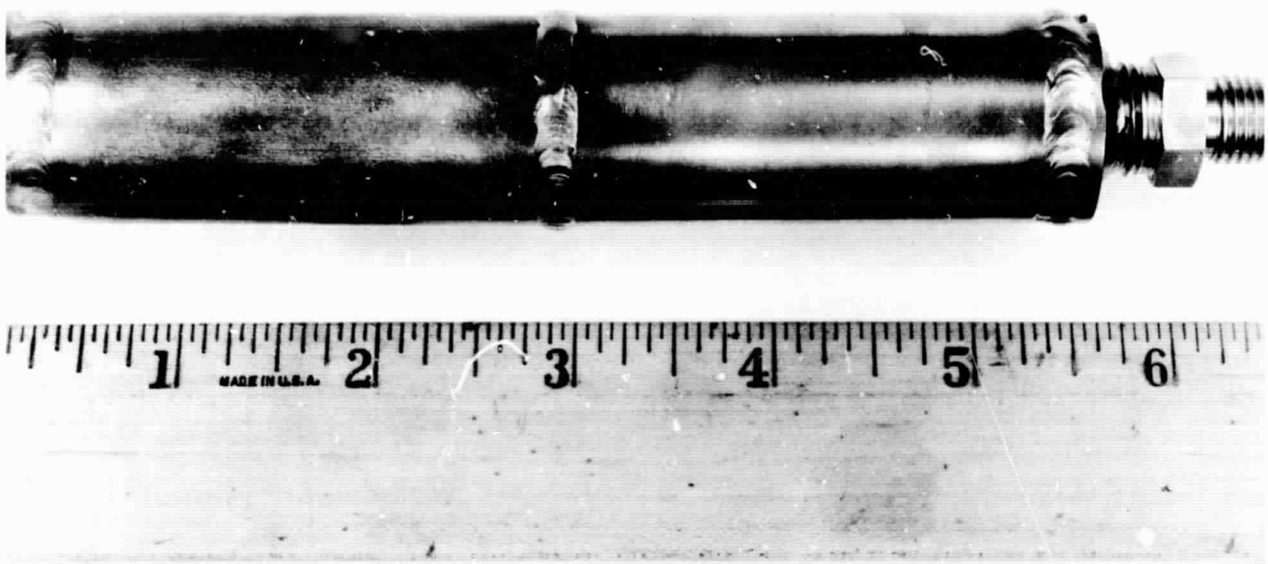

Etchant-
None

Mag. 1X

FIGURE 1: Test capsule used for testing 9Cr-1Mo/316 stainless steel transition joint.

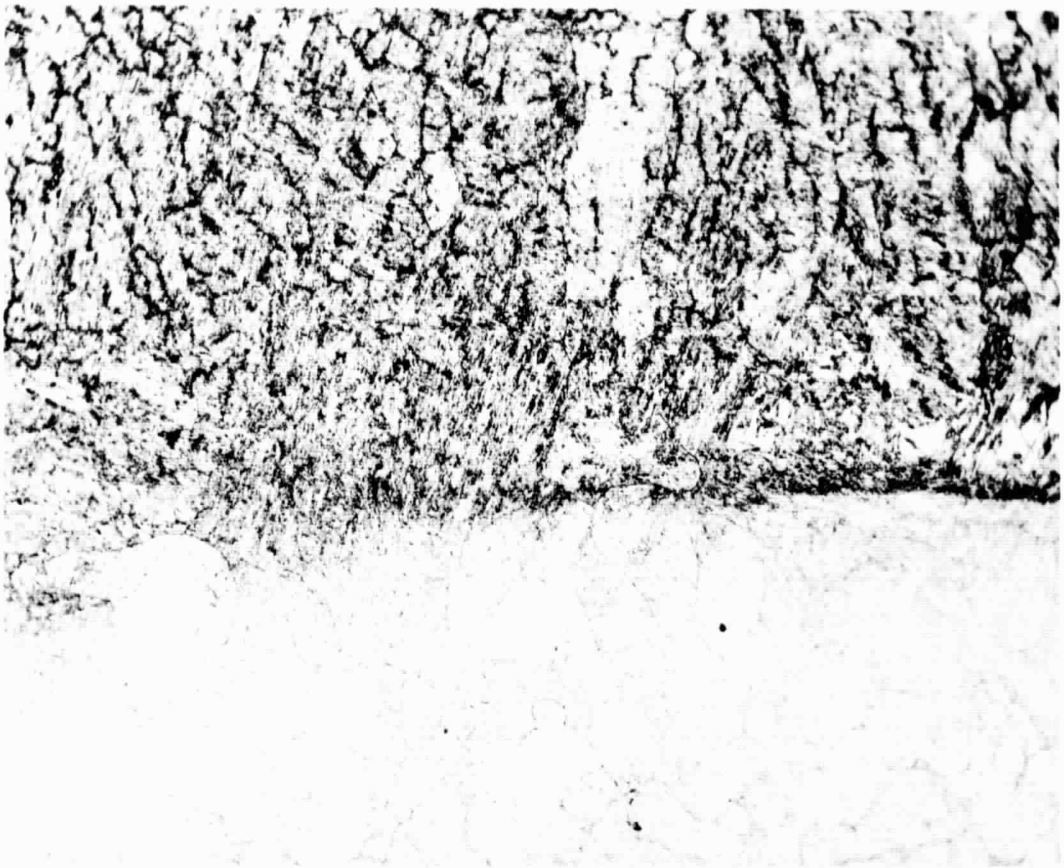

AISI 505 Filler Metal

9Cr-1Mo Parent Metal

Etchant-10% Oxalic Acid

Mag. 250X

FIGURE 2: Interface between 9Cr-1Mo parent metal and AISI 505 filler metal as-welded and stress-relieved.

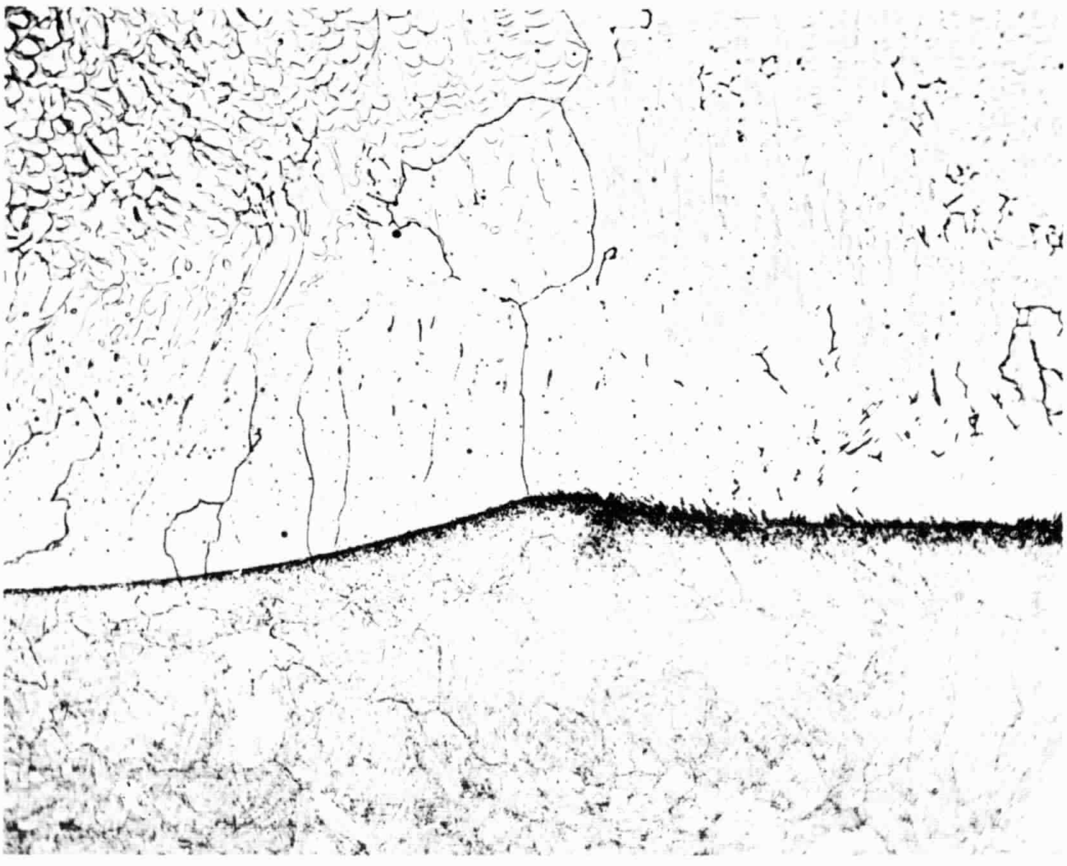

316 L Filler Metal

9Cr-1Mo Parent Metal

Etchant-10% Oxalic Acid

Mag. 250X

FIGURE 3: **Interface between 9Cr-1Mo alloy steel and 316L stainless steel filler metal as welded and stress-relieved.**

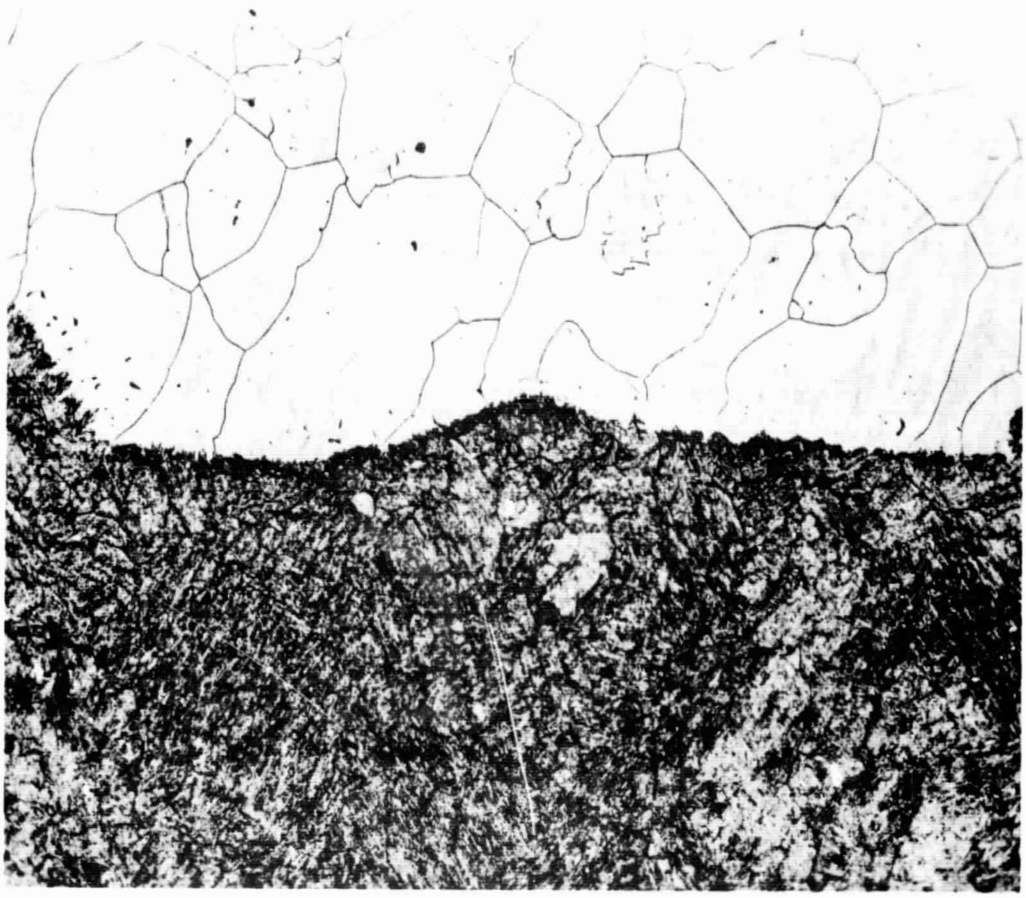

316 Stainless Steel Parent Metal

Etchant-10% Oxalic Acid

AISI 505 Filler Metal

Mag. 250X

FIGURE 4: Interface between 316SS parent metal and AISI 505 filler metal as-welded and stress-relieved.

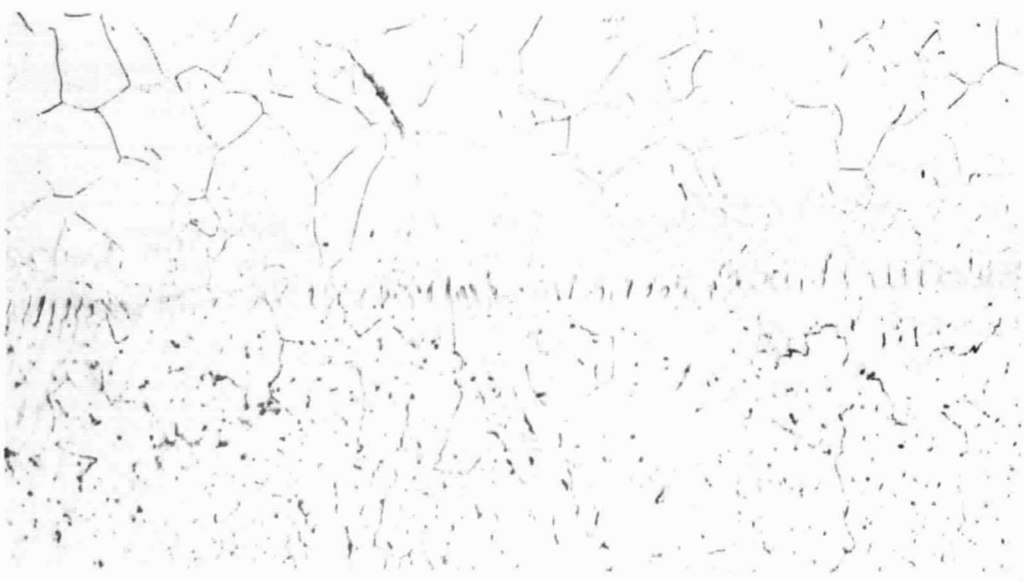

316 Stainless Steel Parent Metal

Etchant-10% Oxalic Acid

Inco A Filler Metal

Mag. 250X

FIGURE 5: Interface between 316SS parent metal and Inco A filler metal as-welded and stress-relieved.

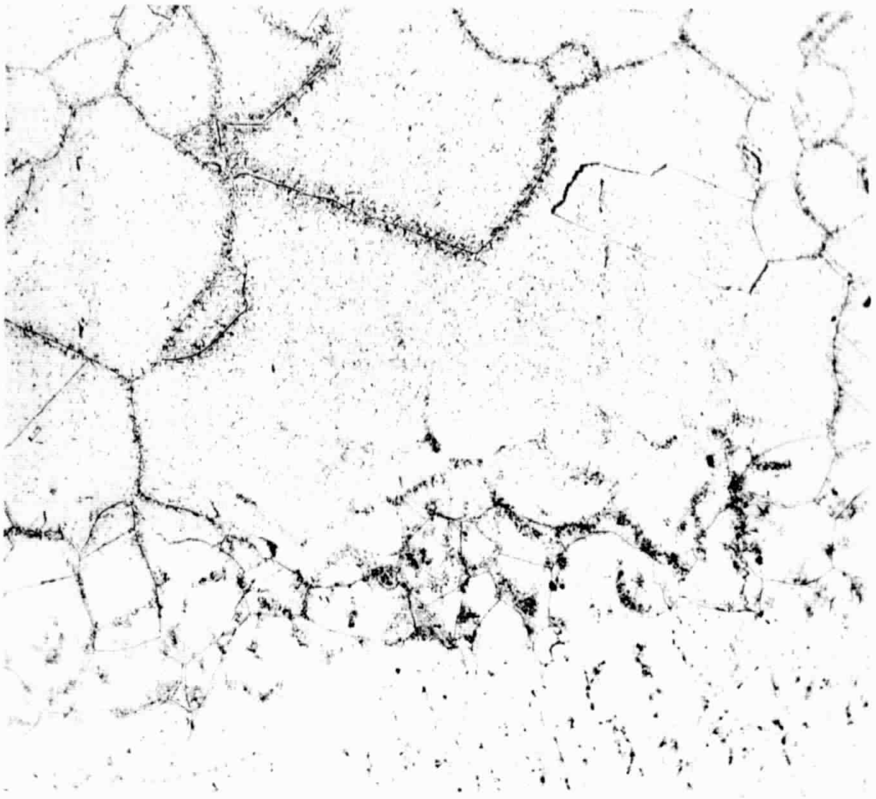

316 Stainless Steel Parent Metal

Excessive Grain Growth in 316 Stainless Steel

AISI 505 Filler Metal

Etchant-10% Oxalic Acid

Mag. 250X

FIGURE 6: Interface between 316 stainless steel parent metal and AISI 505 filler metal after 1871 hours of exposure to temperature pressure cycles, showing fusion line segregation. Carbide precipitation may also be seen in the 316 stainless steel grain boundaries.

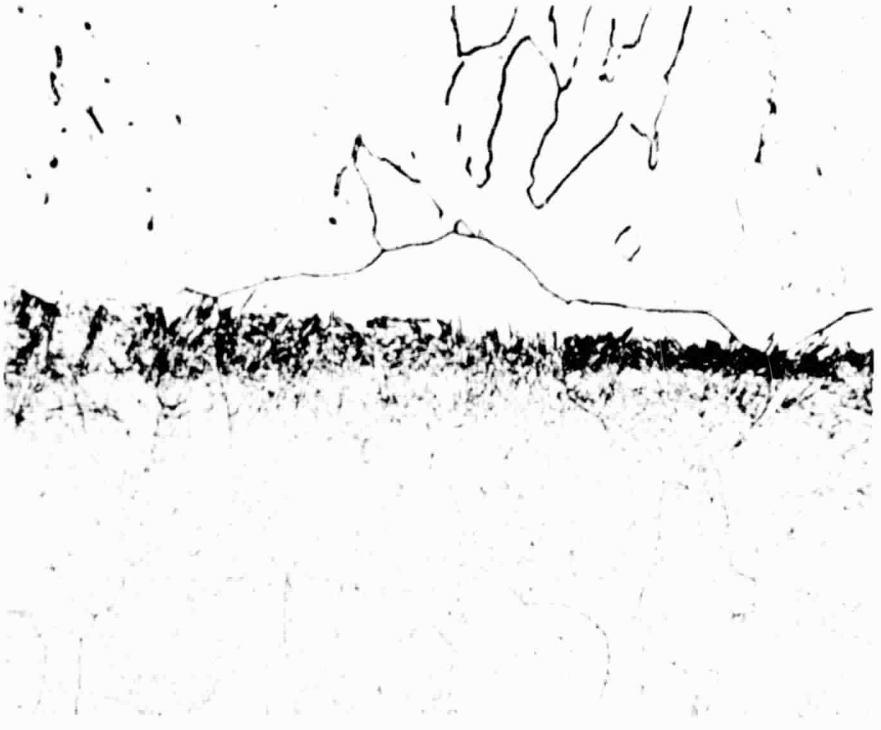

AISI 505 Filler Metal

9Cr-1Mo Base Metal

Etchant-ArmCo Chem

Mag. 250X

FIGURE 7: Interface between 9Cr-1Mo parent metal and AISI 505 filler metal showing fusion line segregation after 1871 hours of exposure to temperature pressure cycles.

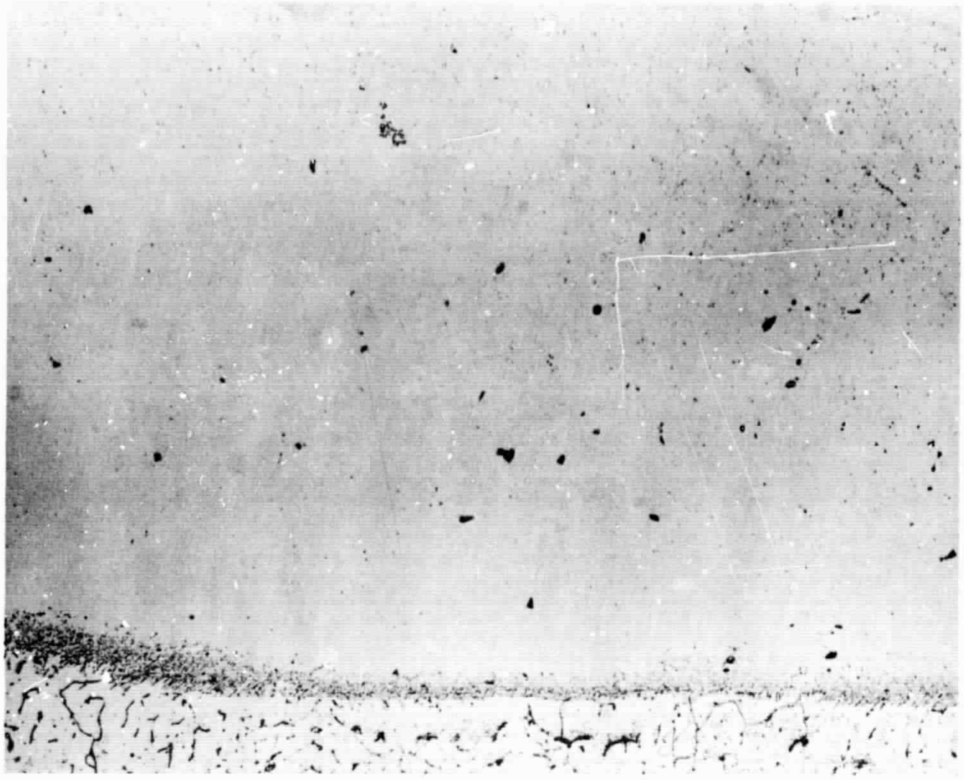

FIGURE 8: Interface between 9Cr-1Mo steel parent metal and 316L filler metal showing fusion line segregation and decarburization after 1871 hours of exposure to temperature.

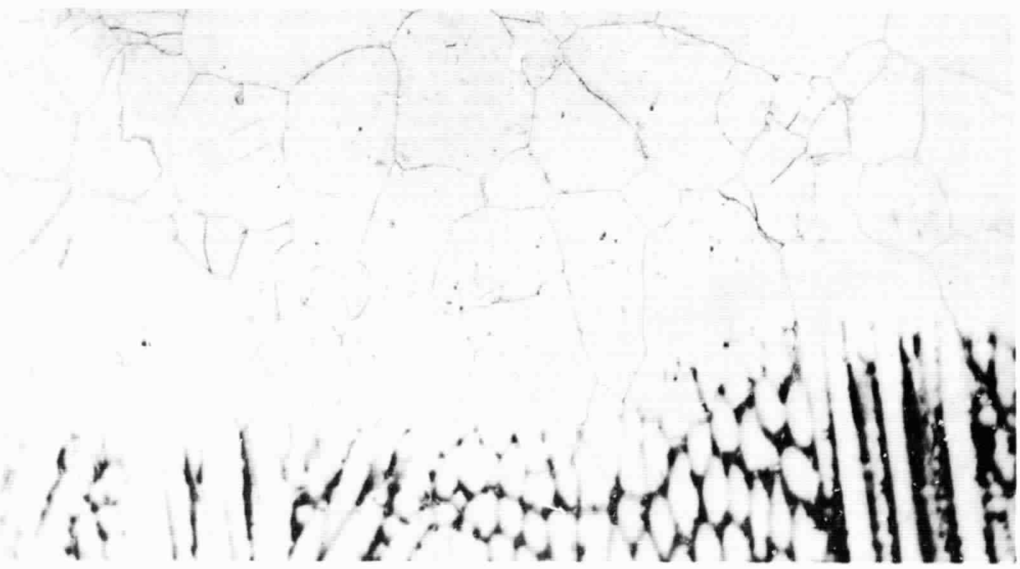

FIGURE 9: Interface between 316 stainless steel and Inco A filler metal showing no segregation after exposure at temperature.

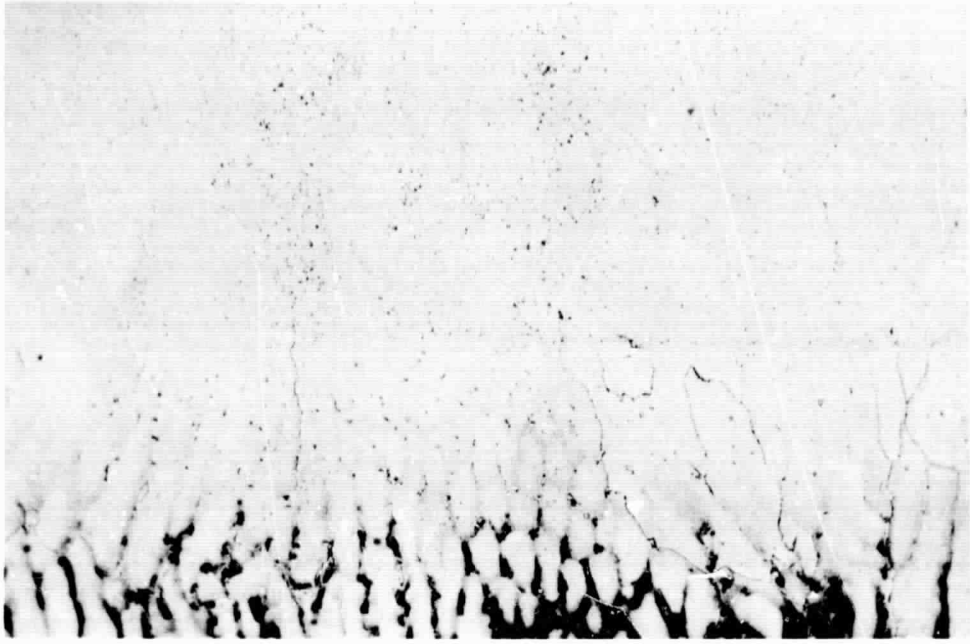

Mag. 250X

FIGURE 10: Interface between 9Cr-1Mo and Inco A Filler showing no segregation after 1871 hours of exposure.

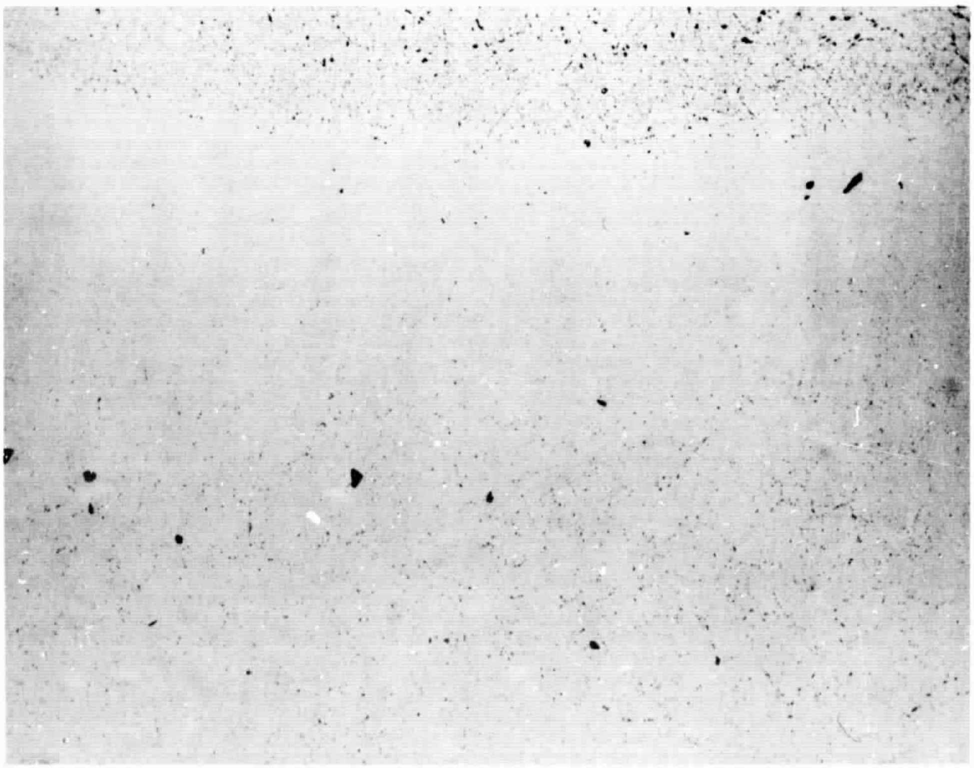

IGURE 11: Interface between AISI 505 filler and 9Cr-1Mo parent metal fusion line showing decarburization in the 9Cr-1Mo parent metal after 1871 hours of exposure.

Mag. 250X

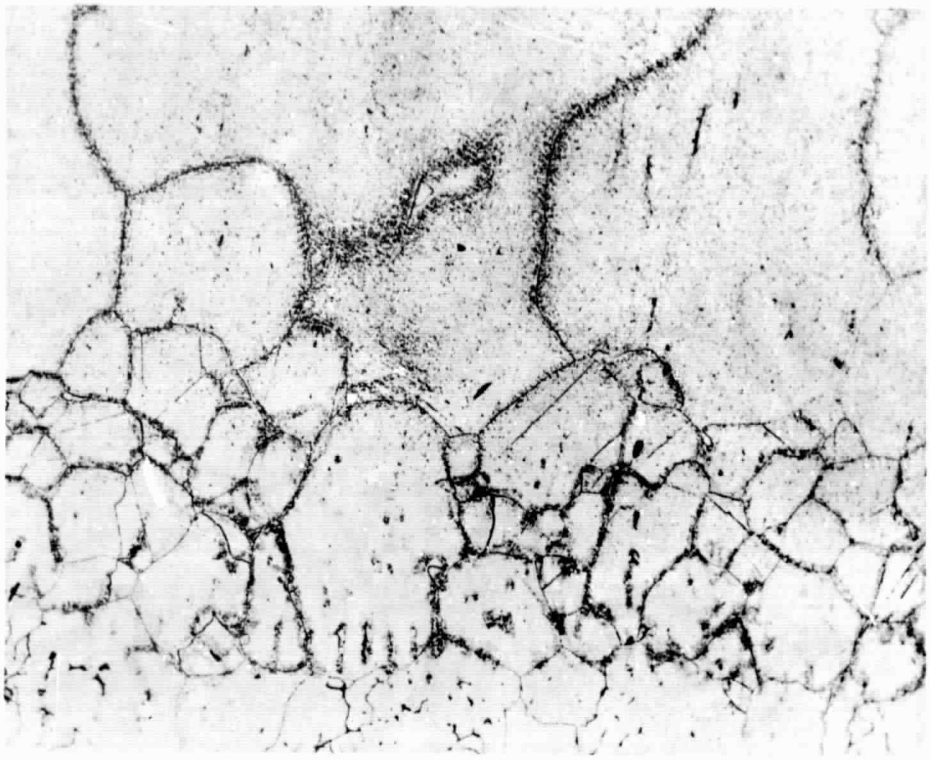

Etchant-10%
Oxalic Acid

Mag. 250X

FIGURE 12: Fusion line between 316L filler metal and 316SS parent metal showing excessive grain growth in the 316 parent metal. Carbide precipitation may also be seen in both the 316SS parent metal and the 316L filler after 1871 hours of exposure.

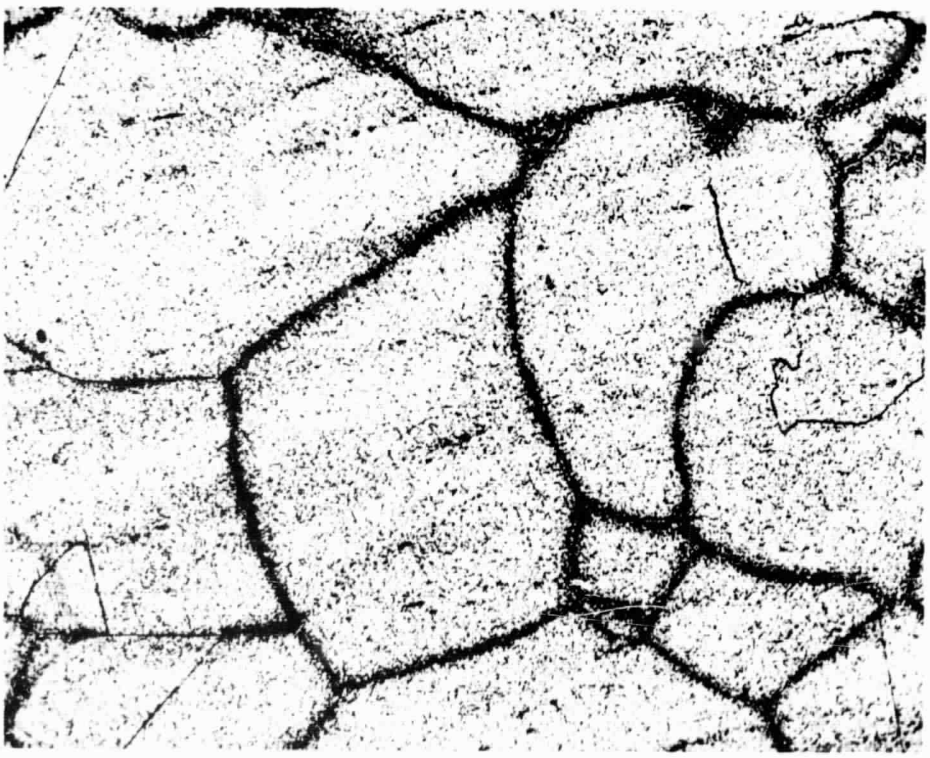

Etchant-10%
Oxalic Acid

Mag. 250X

FIGURE 13: View of 316SS heat affected zone showing excessive carbide precipitation due to heating in the range of 1325-1350°F. Due to volume of consideration, sigma phase (chromium carbide) is suspected as a microconstituent.

Cr-1Mo Parent Metal

316SS Parent Metal

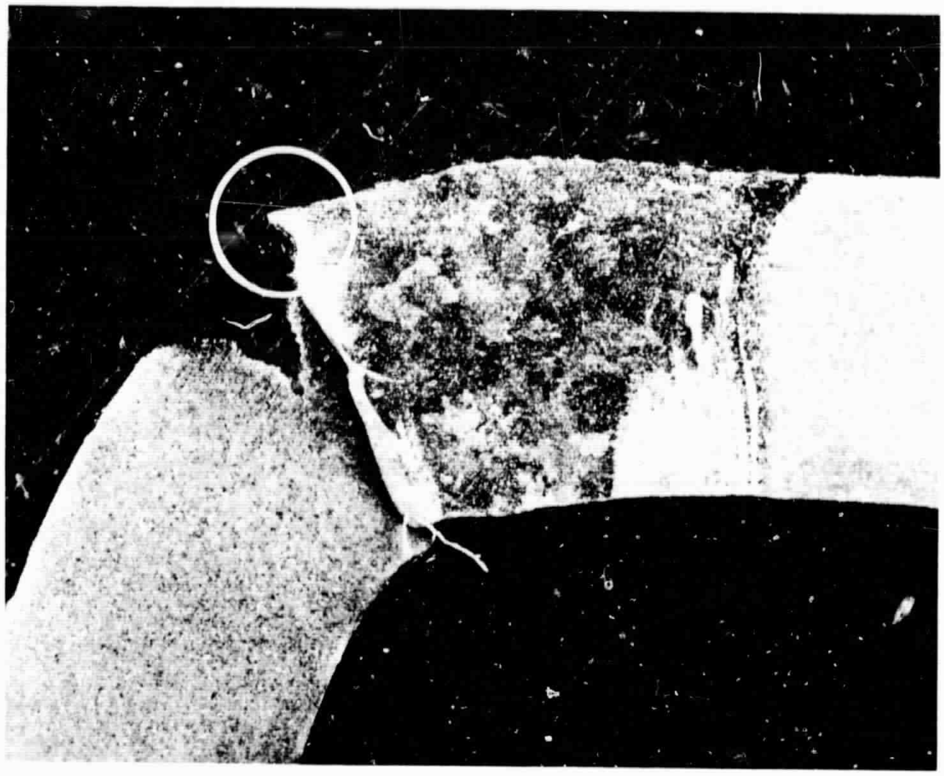

Etchant-10% Oxalic Acid

Mag. 14X

FIGURE 14: Bend specimen after completion of testing. A .25" radius pin was used; crack occurred after bending through 150°.

316 Stainless Steel

9Cr-1Mo Parent Metal

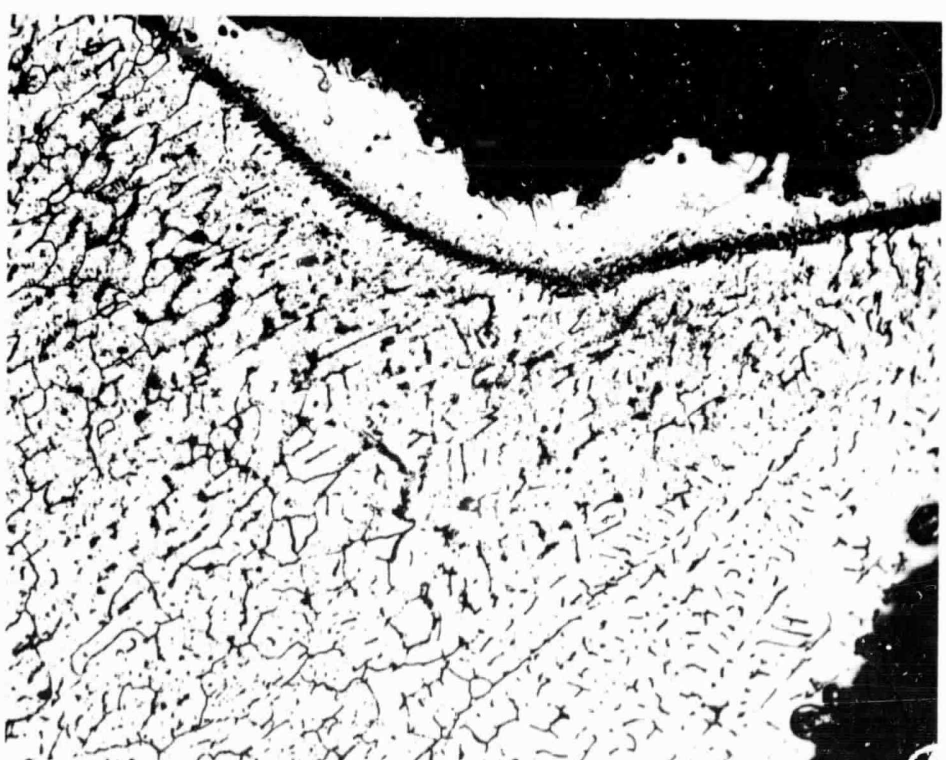

Etchant-ArmCo
em

Mag. 250X

FIGURE 15: View of circled area on Figure 10. Showing segregation at the fusion line and decarburization in the 9Cr-1Mo heat affected zone.

ArmCo Chem

Mag. 250X

FIGURE 16: Detail at base of crack.

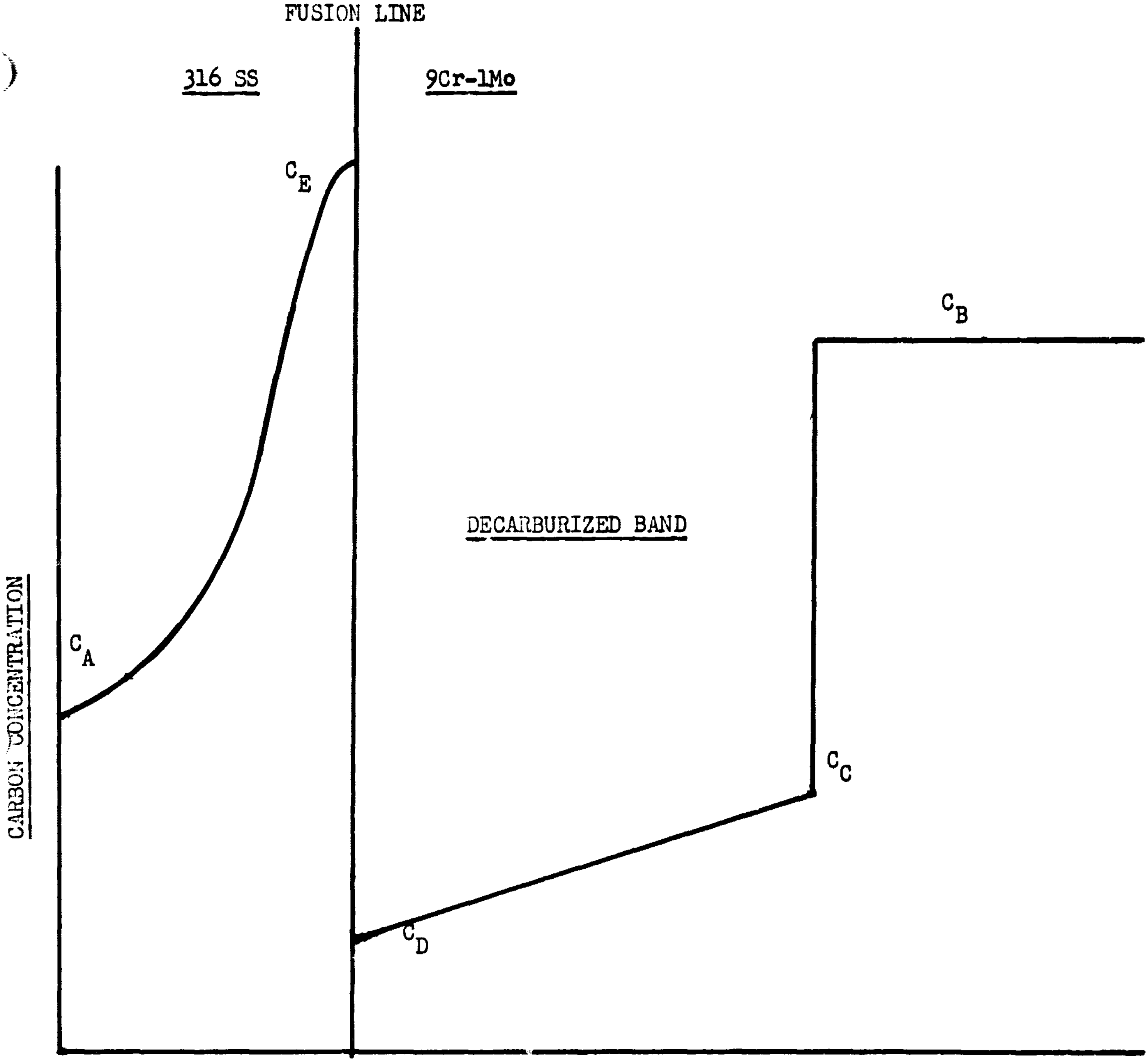

C_A = Original total carbon content in 316SS.

C_B = Original total carbon content in 9Cr-1Mo.

C_C = Carbon solubility concentrated in 9Cr-1Mo.

C_D = Carbon content of 9Cr-1Mo at the fusion line.

C_E = Carbon content of 316SS at the fusion line.

FIGURE 17: Schematic diagram of carbon in composite weldment after exposure for some time interval at an elevated temperature.

NOTE: Modified from Welding Journal, September 1956, Christoffel, Curran - "Carbon Migration in Welds."

APPENDIX A

The following information was taken as an excerpt from "Welding Journal, 1956.""

The progress of the over-all carbon migration progress can then be described as follows:

1. Carbon in solution crosses the fusion line from the low-alloy material to the high-alloy material. The prime driving force which causes the carbon to migrate is the alloy difference between the two steels which results in a lower energy for carbon in the high-alloy steel at a high-carbon concentration than in the low-alloy steel at a lower concentration. A measure of the magnitude of this driving force is the difference in carbon concentration on the high-alloy and low-alloy sides of the fusion line ($C_E C_D$).

2. The addition of carbon to the high-alloy side increases the carbon concentration on this side of the joint and may result in the precipitation of some carbides if the carbon concentration is above the solubility limit. The added carbon will result in a carbon and will tend to migrate away from the fusion line under the influence of this gradient ($C_E C_A$).

3. The carbon which has crossed the fusion line reduces the concentration of the carbon in solution in the low-alloy material. This results in a carbon concentration gradient in the low-alloy material ($C_C C_D$). The carbon diffuses to the fusion line in the low-alloy material under the action of the concentration gradient.

4. When the carbon concentration in the low-alloy material has dropped below the solubility value by virtue of the migration across the fusion line, some of the total carbon which is in the the form of a carbide breaks up and goes into solution (carbon can only migrate when in solution - not as a carbide) to bring the carbon level in solution back up to its solubility value at this point.

It can be seen from the description that the solution of the carbides accounts for the occurence of the decarburized band. Also, it can be seen that the solution reaction occurs only at the plane parallel to the fusion line plane where the carbon concentration in solution has just dropped below its equilibrium value. This accounts for the sharp boundary of the decarburized bank and the sharp break in the total carbon concentration at the boundary.

This is a schematic description of the carbon migration phenomena in composite weldments. The phenomena can be described mathematically, as shown in eq. (1):

$$X^2 = \frac{C_C - C_D}{C_B} 2DL$$

D = Diffusion coefficient of carbon

L = Time

X = Width of the decarburized band

(C_C, C_B, C_D = are defined in Figure 17)

It is possible to show from eq. (1) that the relationship between the temperature and time necessary to produce a given width of decarburization band can be expressed as parameter P which is written as follows:

$$P = K/T + \log L \quad (2)$$

where:

K = Constant

T = Temperature (^{o}Rankine)

L = Time (hour).

REFERENCE PAGE

1. "New Methods of Bonding Dissimilar Materials," F. Zimmer, Bureau D'Estudes Industrielles, Fernand Courtoy, Brussels, Belgium, 1962.

2. Welding Journal, September 1956, Christoffel, Curran, "Carbon Migration in Welds."